NATO OTAN NURC

a NATO Research Centre
un Centre de Recherche de l'OTAN

NURC
PARTNERING FOR MARITIME INNOVATION

**Reprint Series** **NURC-PR-2012-009**

# Antisubmarine warfare applications for autonomous underwater vehicles: The GLINT09 field trial results

Michael J. Hamilton, Stephanie Kemna, David T. Hughes,

May 2012

Originally published in:

Journal of Field Robotics, Vol. 27, No. 6, pp. 890-902, 2010.

# About NURC

## *Our vision*

- To conduct maritime research and develop products in support of NATO's maritime operational and transformational requirements.
- To be the first port of call for NATO's maritime research needs through our own expertise, particularly in the undersea domain, and that of our many partners in research and technology.

One of three research and technology organisations in NATO, NURC conducts maritime research in support of NATO's operational and transformation requirements. Reporting to the Supreme Allied Commander, Transformation and under the guidance of the NATO Conference of National Armaments Directors and the NATO Military Committee, our focus is on the undersea domain and on solutions to maritime security problems.

The Scientific Committee of National Representatives, membership of which is open to all NATO nations, provides scientific guidance to NURC and the Supreme Allied Commander Transformation.

NURC is funded through NATO common funds and respond explicitly to NATO's common requirements. Our plans and operations are extensively and regularly reviewed by outside bodies including peer review of the science and technology, independent national expert oversight, review of proposed deliverables by military user authorities, and independent business process certification.

**Copyright © Wiley, 2010.** NATO member nations have unlimited rights to use, modify, reproduce, release, perform, display or disclose these materials, and to authorize others to do so for government purposes. Any reproductions marked with this legend must also reproduce these markings. All other rights and uses except those permitted by copyright law are reserved by the copyright owner.

**NOTE**: The NURC Reprint series reprints papers and articles published by NURC authors in the open literature as an effort to widely disseminate NURC products. Users are encouraged to cite the original article where possible.

# Anti-Submarine Warfare Applications for AUVs: The GLINT09 Sea Trial Results

**Michael J. Hamilton*, Stephanie Kemna, David Hughes**

NATO Undersea Research Centre

Viale San Bartolomeo 400

19126 La Spezia, Italy

hamilton@nurc.nato.int

## Abstract

Surveillance in anti-submarine warfare (ASW) has traditionally been carried out by means of submarines or frigates with towed arrays. These techniques are manpower intensive. Alternative approaches have recently been suggested concerning distributed mobile and stationary sensors, such as sonobuoys and autonomous underwater vehicles (AUVs). To field a fully operational system many technological hurdles need to be overcome. These include battery life, limited acoustic communications ranges, incorporating sonar signal processing on the AUVs embedded hardware and increasing autonomy to ensure that the system as a whole acts in a sensible and appropriate fashion. The main thrust of this paper is how the latter two issues have been addressed for a real experimental system and how the proposed solutions have been demonstrated at sea.

*Address from USA/Canada: NURC, CMR 426 Box 681, APO, AE 09613-5000.

This paper describes on-going development at the NATO Undersea Research Centre (NURC) to construct an autonomous distributed sensor system that uses AUVs for ASW applications. In a series of at sea experiments we have demonstrated real-time processing - incorporating traditional ASW processing as far as tracking - and adaptive autonomous behaviors, which concern AUV navigation to optimize target localization. This paper describes the hardware and software configurations that facilitated the rapid development of this system and details the recent at sea successes that have been demonstrated with our AUV, towed arrays and active acoustic sources. Results are given of our most recent at-sea trial, GLINT09, held in the summer of 2009, when an AUV with a towed array detected and maneuvered in response to an active source.

# 1 Introduction

Traditionally the task of anti-submarine warfare (ASW) is a manpower and computationally intensive discipline. Various levels of sophisticated sensors gather large amounts of data, for example from towed arrays or sonobuoys, from which the relevant information, in terms of possible targets, threats, or false alarms, must be extracted. From this information a decision must be inferred by an operator or commander and a consequent action taken. Should the detection be ignored? Should it be passed on for further analysis? Should it be acted on directly, for instance by deploying a helicopter with a dipping sonar as a step towards the ultimate prosecution of the target?

We are investigating an alternative approach to traditional anti-submarine warfare. Rather than performing ASW with a single, large, high capability, capital ship or submarine working individually (or with limited joint operations, e.g. a helicopter), we are investigating the concept of employing a system of many, small, limited capability, low-cost systems working

in concert. In this case the sensors and underwater assets make collaborative decisions independent of an operator and carry out the necessary changes to their actions. The first goal in introducing this kind of autonomy is to optimize the detection, classification, and localization of a target. Of course, in order to make these decisions in real time, data processing must also be completed in real time. Processing on-board these small vehicles is typically limited by vehicle size, heat generation, and power constraints. A limited set of signal processing algorithms, compared to those which can be run on-board a large ship or submarine, must be chosen so that processing is possible without overly sacrificing performance. The sensors to be used for this kind of work may be bottomed non-acoustic sensors such as hydrophones or magnetometers or mobile systems such as gliders or powered AUVs pulling towed arrays. All technologies bring their own advantages and problems. We have focused on an AUV/towed array approach and the technology is described in Section 2.1.

The use of AUVs for ASW is a recent approach and not many research groups concern themselves with this field. Previous work has discussed vehicle control without processing (Benjamin et al., 2007), passive processing with an AUV using a nose-mounted array (Poulsen et al., 2006), or the use of kayaks, rather than AUVs, for 2D target tracking (Eickstedt and Benjamin, 2006). The feasibility of multistatic processing and tracking with AUVs has also been discussed (Lum et al., 2009), but the provided data was processed off-board. To the best of our knowledge, active sonar processing on board an AUV and subsequent use of the processed data has thus not been shown before.

Outside of ASW, most research has taken place into AUV navigation; among others concerning efficient path planning, both in the field of mine counter-measures and oceanography (Pêtrès et al., 2007; Kruger et al., 2007; Williams, 2010). Research has also focused on making AUVs more adaptive to the environment, for example using simultaneous localization and mapping (SLAM) (Newman et al., 2003; Eustice, 2005; Barkby et al., 2009), and making them more adaptive to other vehicles through coordinated navigation and localiza-

tion (Alvarez et al., 2009; Kalwa, 2009; Bahr et al., 2009).

During the GLINT09 (Generic Littoral Interoperable Network Technology) sea trial, we overcame many of the previously mentioned hurdles and demonstrated an autonomous underwater vehicle (AUV) responding to towed array sensor data processed on-board the vehicle in real time. Our current system consists of a bi-static active sonar, relying on our previously developed expertise in, and equipment for, multistatic sonar and ASW (Ehlers, 2009). In a bi-static sonar, the source and receiver are spatially distributed. In our test we utilize a stationary, buoy mounted sound source. The receiver was a towed array pulled by our AUV. Our AUV was programmed using the MOOS-IvP (Mission Orientated Operating Suite-Interval Programming) software suite developed by our collaborators at the Massachusetts Institute of Technology (MIT), Naval Undersea Warfare Centre (NUWC), and Oxford University (Benjamin et al., 2009). MOOS-IvP provides the basic infrastructure and autonomy control for this system. To that, we have added our own suite of sensor signal processing and two adaptive behaviors.

This paper is laid out as follows: Section 2 gives an overview of the the GLINT09 sea trial, and the equipment and algorithms used are explained and parametrized in detail. In Section 2.3 specific details of the settings used in the sea trial are described. Section 3 shows results from the sea trial and comments are made on expected and obtained results. Conclusions are given in Section 4. Section 5 comments on some of the limitations in our current approach and how we intend to reconcile those over the next year.

# 2 Description of the GLINT09 sea trial

The GLINT09 sea trial was held between 29 June and 18 July 2009. The experiment took place in an area to the south-east of the island of Elba, close to the Formiche Islands off the coast of Italy. The area was ideally suited to an AUV based experiment because of its

relatively flat bathymetry at a depth of approximately 110 meters.

Our primary platform of operations was the NATO research vessel NRV Alliance. The AUV was deployed and recovered from the Alliance daily. Additionally, our command center was set up in the lab area of the ship. Our sonar source, described below, was deployed from the Alliance and left in place for the duration of the trial. Also present was the coastal research vessel CRV Leonardo, which was used to tow an echo repeater target simulator for testing of the multistatic processor.

The goals of the experiment included a great deal of testing and data collection during the early stages. The ultimate objective, however, was to demonstrate an adaptive behavior on the AUV which uses the outputs of the real-time signal processing. At this early stage the demonstration was somewhat contrived. We utilized a high source level and had the AUV respond to the direct blast of the source, rather than responding to the target echo as is typical in sonar. Because the source was stationary and very high level, it enabled us to test the autonomy algorithm against an "easy", high signal-to-noise ratio (SNR) target. We successfully performed true real-time bi-static sonar processing against the echo repeater test target towed by Leonardo, but did not couple that with the autonomy at this time.

The following sections describe the experimental equipment and processing algorithms used during the trial. Processing is described first in a general, parametrized sense. Then, the parameters and exact settings used during the trial are described.

## 2.1 Equipment

### 2.1.1 OEX AUV with SLITA towed array

The main tool of research for the GLINT09 trial was NURC's Ocean Explorer (OEX) AUV used in combination with NURC's **SL**im **T**owed **A**rray (SLITA). The OEX is an untethered

AUV of 4.5 meters length and a diameter of 0.53 meters (21"). It can operate to a maximum depth of 300 meters. It has a maximum speed through the water when towing the array of 3 knots. Current battery constraints limit the lifetime of any mission to about 7 hours. The OEX is equipped with two independent modems. One of these is a Wood Hole Oceanographic Institution (WHOI) modem (Freitag et al., 2005) which was used for communication of data with the command center. The second is an EdgeTech acoustic modem integrated with the vehicle main computer that sends vehicle location information only.

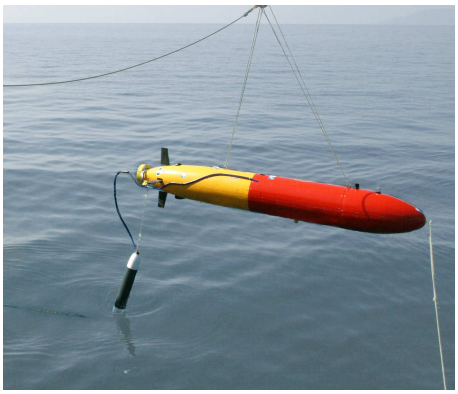

Figure 1: OEX AUV being lowered into the water. The towed source can be seen dangling behind the AUV, and further behind looping through the water is the start of the SLITA towed array.

The OEX AUV is shown in Figure 1 with the attached SLITA array. The SLITA array used was actually an upgraded version of the one described in (Maguer et al., 2008). The array has a total of 83 hydrophones, with sets of 32 selected at any given time. There are four sets configured for optimal frequency spacings from 714Hz (105.0cm) to 3471Hz (21.0cm). This range of frequencies allows us to operate in a passive lower-frequency mode as well as in an active, higher-frequency mode. The acoustic section starts 9 m behind the vehicle.

The array is also equipped with three compasses and two depth sensors that aid reconstruction of the array dynamics. Additionally, there is an active source which integrates with the array and can be towed by the AUV (as shown in Figure 1), allowing for future monostatic experimentation.

The OEX AUV itself is equiped with a main computer which directly commands the OEX's control surfaces and maintains navigation. This main computer is capable of controlling the OEX for pre-planned autonomous missions, and for receiving basic commands via acoustic modem, which can order the OEX, for example, to abort a mission and surface. The LonTalk protocol is used by the vehicle computer for internal vehicle command and control messages.

The OEX also has a configurable mission payload section. The configurable payload section utilized in GLINT09 is shown with the pressure housing open in Figure 2. It consists of two computer systems set up as pc-104 *stacks*: one for data acquisition from the SLITA array, the other for signal processing and MOOS-IvP autonomous decision making. The assignment of data acquisition to one computer and processing to the other is somewhat arbitrary, but is focused to provide ample processing power for data acquisition.

The pc-104 main boards in each stack have single core 1.4GHz Pentium-M processors with 1GB of RAM on board. These computers both run Linux operating systems, which aids in rapid development and ease of integration, even if not strictly a real time operating system. In our case, "real time" with respect to the data processing implies that processing is completed faster than new data comes in, and therefore can keep up with incoming data. The two payload computers are connected via Ethernet to each other, and via LonTalk to the vehicle main computer.

Figure 3 shows a schematic of this system. Data comes in from the SLITA array on 32 channels, one for each active hydrophone, through the A/D board, which is connected to the pc-104 acquisition stack via a PCI interface. Data is archived on the local acquisition computer's hard drive, and also transferred via standard network file system (NFS) protocol to the hard drive connected to the MOOS/processing stack.

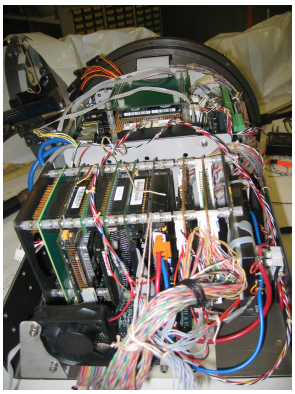

Figure 2: OEX payload section for SLITA array system. The cylindrical pressure housing is removed. The nearer pc-104 *stack*, laid horizontally in the photo, is the data acquisition portion of the processing payload, and has a digital acquisition card connected to the stack (partially visible beneath wires and fan). The farther pc-104 *stack*, laid out vertically in the photo (only the top is visible), performs the MOOS-IvP and signal processing.

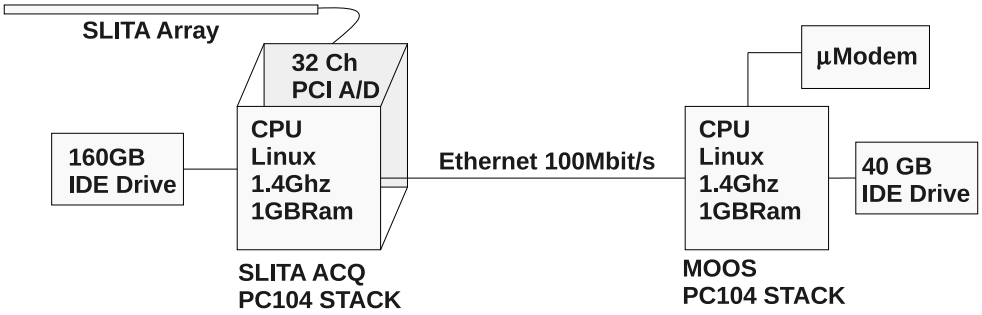


Figure 3: Payload computer diagram for the GLINT09 test. The SLITA array in the diagram was the upgraded SLITA array for GLINT09. The $\mu$Modem in the diagram is a WHOI acoustic modem attached to the processing stack.

### 2.1.2 DEMUS acoustic source

The distributed multistatic underwater surveillance (DEMUS) source, shown in Figure 4, is a programmable bottom-tethered acoustic source based on free-flooded ring technology. It has a maximum source level of 217 dB, and a programmable acoustic frequency range from between 2 and 4.2 kHz. A radio buoy floats on the surface attached to the source so that the acoustic signals to be transmitted can be altered by means of a radio connection. The radio buoy also has a GPS which provides very accurate transmission timing and source position localization. Accurate timing and localization of the source are critical inputs for accurate

bi-static sonar processing.

The acoustic source is also equipped with a WHOI acoustic modem which allows it to be turned on and off remotely by means of acoustic communications. This allows our AUVs to trigger the source to start pinging, for example after making a passive detection. This particular capability was not used in this trial, although we have effectively tested it.

Figure 4: The DEMUS acoustic source being deployed (left). The eight free-flooded transducer rings are visible on top, with the electronics canister underneath. The DEMUS surface buoy (right) is shown during a battery replacement. GPS and radio command antennae are visible on top.

## 2.2 Algorithms and software implementation

### 2.2.1 MOOS-IvP

The signal processing and decision-making engine utilized MOOS-IvP as its underlying software infrastructure. MOOS-IvP has two primary functionalities (Benjamin et al., 2009). First, it provides a basic suite of AUV autonomy processes for navigation, control, acoustic communications, etc. The IvP-helm process in this suite specifically enables the use of multiple "behaviors". Different behaviors (e.g. obstacle avoidance or course following) are active at the same time and their weighting determines their importance towards the output. IvP-helm combines the objective functions of each behavior to determine AUV heading, speed and depth (Benjamin, 2004).

The second function provided by MOOS is interprocess communications (IPC). Information can be shared between processes through a publish-subscribe structure to the MOOS database (Benjamin et al., 2009). By providing this middleware layer of communication, new processes may be added quickly and easily, and may interact with legacy processes or replace them. The MOOS database also provides for convenient logging of data. All messages published to the database can be archived, along with timestamps and process of origin name.

The MOOS-IvP helm control integrates with the OEX vehicle using a "front-seat driver/back-seat driver" paradigm, as shown in Figure 5. The OEX vehicle main computer acts as the "front-seat driver", directly manipulating the vehicle control surfaces, maintaining trim, etc. The payload computer, specifically the MOOS/processing stack described in 2.1.1, acts as the "back-seat driver". MOOS-IvP decides the direction, speed and depth for the vehicle. This can be the result of mission parameters, the IvP behavior solutions, and the real-time data acquisition and processing. The desired heading, depth and speed are sent to the front-seat driver computer, which then actually performs the necessary maneuvering. This model provides for a convenient fail-safe should the back-seat driver computer fail or begin to drive the vehicle out of area. The vehicle main computer can also be cued via acoustic modem to ignore back-seat driver commands, or it may take over and make the AUV return to base or surface should it cease to receive information from the back-seat driver.

At NURC we are building on the infrastructure provided by MOOS-IvP. We have introduced a real-time signal processing capability which analyses every ping, forming contacts and ultimately forming tracks. The implementation of a fully functioning active ASW signal processing chain on a PC104 stack has been a challenge and the steps taken to make it possible are detailed in the next section, 2.2.2.

With the sonar signal processing in place the algorithm designer can start to consider how the

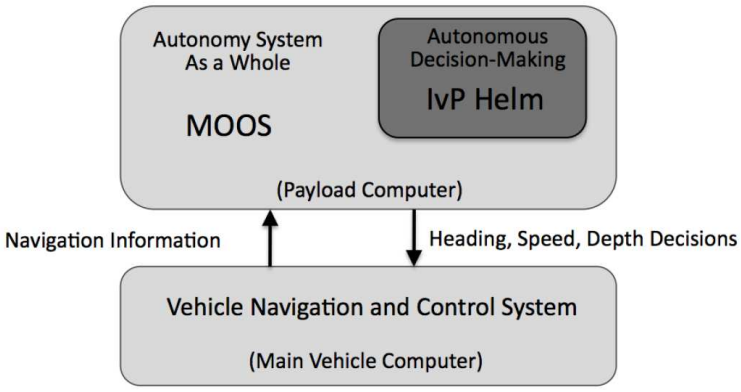


Figure 5: **The backseat driver paradigm**: The key idea is the separation of vehicle autonomy from vehicle control. The autonomy system provides heading, speed and depth commands to the vehicle control system. The vehicle control system executes the control and passes navigation information, e.g., position, heading and speed, back to the autonomy system. The backseat paradigm is agnostic regarding how the autonomy system is implemented, but in this figure the MOOS-IvP autonomy architecture is depicted working with the vehicle main computer as the control system (Benjamin et al., 2009)

.

AUV should react to its world view. In Section 2.2.3 we discuss, in detail, a simple adaptive behaviour which illustrates what can be done and we discuss how it was demonstrated at sea.

### 2.2.2 Sonar signal processing

The signal processing suite was developed using a combination of algorithms and previous software by MIT for similar active sonar processing (Lum et al., 2009) and from NURC's previous multistatic processors (Laterveer, 2003; Baldacci and Haralabus, 2006). The implemented signal processor is a frequency-domain, configurable band, conventional beamformer and matched filter library for a line array. A MOOS-IvP front end interface, *pProcessSlita*, was created for this library to allow the publication of acoustic detections to the MOOS database. This section gives a general description and parametrization of the algorithm employed. Details on the settings used for the experiments are given in Section 2.3.

Data for each channel (or hydrophone) of the receiving array is recorded into a file at the

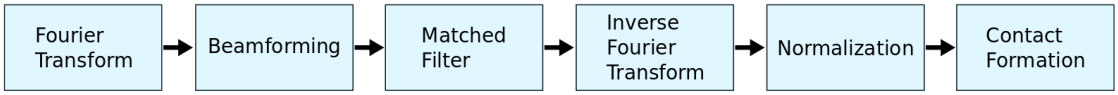


Figure 6: Standard signal processing chain of events: beamforming, matched filter, normalization and contact formation. Each box is detailed in this section.

sampling rate. The data file is then moved from the acquisition stack to the processing stack as described in Section 2.1.1. The signal processor detects the creation of the new file and reads it into memory. Array/hydrophone data was not transferred through the MOOS database, as MOOS is designed to handle text-based messages or short data transfers. The large data bandwidth required for the hydrophone data made direct reading from the file more efficient.

Once the file is read, the processor moves through the following signal processing stages, as depicted in Figure 6 and further detailed in the rest of this section: Fourier transform to frequency domain, frequency domain beamforming, matched filtering using overlap-save method, inverse Fourier transform, along-beam (1-D) normalization, and contact formation.

**Fourier transform**

The data is first transformed into the frequency domain. Since the data timeseries is real valued, the discreet Fourier Transform is Hermitian symmetric. This means that only the positive frequencies need to be computed and processed, the negative frequencies being redundant. The transform was performed using the Fast-Fourier Transform (FFT) in the Newmat library (Davies, 2006) during the GLINT09 sea trial, but has subsequently been upgraded to the FFTW library (Frigo and Johnson, 2005).

FFT's are performed in overlapped segments or "snapshots". The overlap length is dictated by the overlap-save method to be the length of the matched filter (Proakis and Manolakis, 1996). In this case, the 1-second length of the active sonar pulse is used. The length of the FFT itself is configurable. Given trade-offs in FFT processing vs. overlap length, (Borgerding, 2007) suggests a power-of-two FFT length about four times the length of the

matched filter, but this should be tested on target hardware to find the fastest FFT length. The first segment is zero padded at the beginning by the overlap length. This end effect is accounted for by overlap with the subsequent segment.

**Beamforming**

Beamforming is performed in the frequency domain over a selected band. Conventional frequency-domain beamforming is used as described by (Johnson and Dudgeon, 1993). In each of the equations below, the frequency $\omega$ processed included only the selected band $\omega = [\omega_c - BW/2 : \omega_c + BW/2]$, where $\omega_c$ is the center frequency and $BW$ is the bandwidth of the active pulse. Beam pointing directions can be cosine spaced or linear. Cosine spacing is often used since main lobe width is constant in cosine space for a conventional beamformer using an equally spaced line array.

Frequency domain beamforming is computed as

$$B(\theta, \omega) = \sum_{m=0}^{M-1} X(m, \omega) S(\theta, \omega, m) \tag{1}$$

where $B(\theta, \omega)$ (capital $B$ used to denote a frequency domain quantity) is the beamformer output for radian frequency $\omega$ steered in the direction $\theta$, $X(m, \omega)$ is the frequency domain data for array element $m$. The term $S(\theta, \omega, m)$ are the frequency domain steering coefficients or phase shifts defined by

$$S(\theta, \omega, m) = e^{\frac{-jcos\theta\omega\Delta_m}{c}} \tag{2}$$

where $\Delta_m$ is the distance of each array element $m$ from the phase center of the array, and $c$ is the sound speed. Note that Equation 2 is frequently expressed in terms of the wavenumber $k$, which is simply $\omega/c$ in the equation above.

For efficiency during the running of the processor, these frequency domain complex steering coefficients are precomputed at initialization for each beam pointing direction.

**Matched filter & inverse Fourier tranform**

The matched filter is implemented with the overlap-save method. After matched filtering, data is transformed back into the time domain using the inverse Fourier transform. Overlapped portions are discarded as per the overlap-save method. This process repeats until not enough new data remains in the file for another complete segment to be processed. The rest of the data is discarded, resulting in a small data loss at the end of each file. The exact amount depends on the the selected FFT sizes, overlaps, and length of time series in the file. This loss could be mitigated by saving the data over time from sequential files, and continuing the overlap-save process. Indeed, this type of continuous processing capability was initially envisioned, but at this time was not required or implemented.

**Normalization**

The data is now in the form of matched filter output beam timeseries. Normalization is performed in the time domain down each beam with a split-window method normalizer as described in (Baldacci and Haralabus, 2006). For each point in the time series, leading and lagging sample windows are used to compute the mean noise level. A guard band separates the sample to be normalized from the noise estimation window to avoid signal contamination in the noise estimate. The data point is normalized by the computed mean noise in the noise estimation windows. At the beginning and end of the time series, these windows are smaller due to the end effects. For example, the first sample has only the noise estimate from the leading window. As the windows are applied to data at increased distances from the beginning of the file, the noise estimate from the lagging window is gradually added. Similar effects occur at the end of the timeseries.

**Contact formation**

Once we have the normalized timeseries, we utilize a very simple detector/classifier: The

three highest SNR range-bearing points are returned by the processor. The strongest range-bearing point is selected and output as the first contact. Since a detection usually consists of several range-bearing points in a cluster, data along that range and beam (bearing) are then masked out. The process is then repeated with the second and third strongest range-bearing points. This process of masking is a simplistic version of solving the clustering problem, preventing multiple detections from forming on the main response lobe of a single actual target. However, as a result, only one detection can be found on any given bearing or at any specific range. This crude contact formation/classification method was adequate during GLINT09 for proof-of-concept. The vehicle was tasked to track the source, which was always the strongest contact, or the echo repeater, also set with high levels and therefore always the second strongest contact. In the future we intend to implement a constant false alarm rate (CFAR) style algorithm for this process, similar to the one in (Baldacci and Haralabus, 2006).

Some of the processes in the MOOS infrastructure for GLINT09 are schematically shown in Figure 7. The processing chain, as previously discussed in this section, is containted in the "pProcessSlita" box. The processor publishes contacts to the MOOS database, including their range, bearing, and SNR values, via a `CLUSTER_REPORT`. The process "pBistaticLocator" geo-locates the clusters by solving the bistatic equation (Coraluppi, 2006), and republishes them to the MOOS database as $(x, y)$ locations on the locally defined operational grid, as well as latitude and longitude. These data were used for plotting in the command center and other visualizations.

Our behavior operates on the SNR and bearing measurements directly. The "clusterReport-ToBHV" process selects the highest SNR contact, and passes its respective SNR and bearing information to pHelmIvP. The pHelmIvP process manages various behaviours, one of which utilizes the information from the selected contact to make navigation decisions. Details are futher described in the next section ( 2.2.3).

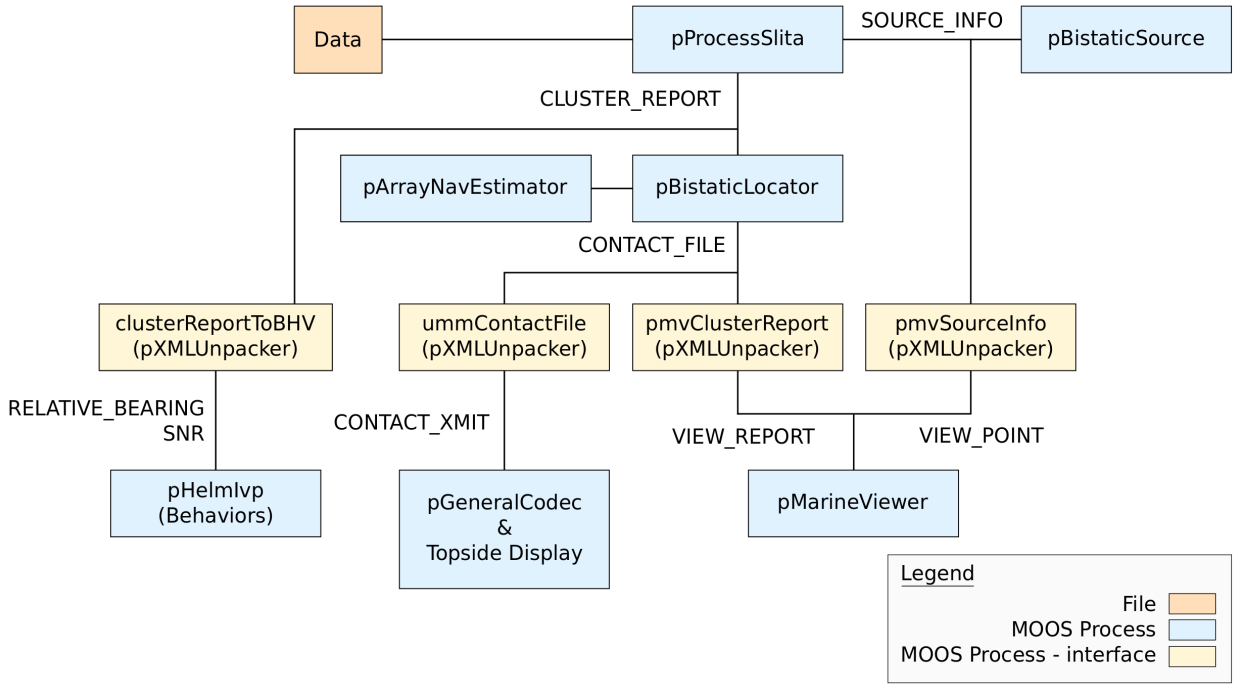


Figure 7: Processing stream for MOOS-IvP implementation on-board the OEX vehicle. All processes in the diagram are running on the MOOS/processing stack. Data is read in 12 second recorded files and processed in pProcessSlita (Figure 6). Data clusters (detections in (range,bearing)) are sent downstream via a MOOS variable (`CLUSTER_REPORT`) to the behaviors (Figure 8) and to the bistatic computation, which creates geo-located contacts in (X,Y) for various display processes.

### 2.2.3 Behaviors

The behaviors are developed within the MOOS-IvP software framework described in Section 2.2.1. The behavior parameters are specified in a behavior file, which itself is referenced in the pHelmIvP process configuration block of the overall mission configuration file. These mission configuration files are loaded onto the OEX payload computer before deployment.

Two behaviors were developed for the GLINT09 sea trial: an adaptive loiter and an adaptive broadside behavior. The term "broadside" refers to the target bearing relative to the acoustic array. In the case of a vehicle towing an array straight behind it, broadside is 90° relative to the heading of the vehicle. When a target is at broadside to the array, the full aperture of the array is applied to resolve the bearing. Conversely, a target at or near "endfire",

i.e. directly behind (bearing 180°) or in front of (bearing 0°) the array, will have a poorly resolved bearing (Sindt and de Theije, 2003; Hughes et al., 2008). Essentially, then, the goal of the broadside behavior is to turn the array in order to produce the best bearing resolution.

**Adaptive loiter**

The *adaptive loiter* behavior is an adaptation of the standard loiter behavior that is part of MOOS-IvP (BHV_Loiter in (Benjamin et al., 2009)). The standard loiter behavior sets waypoints for the vehicle using a closed path polygon. The vehicle drives around this polygon repeatedly. The *adaptive loiter* differs from a standard loiter by examining the highest SNR contact in the MOOS database as it drives in this polygon pattern. If the SNR value of that contact is being actively updated and exceeds the *SNR threshold* parameter, the AUV will switch to the mission specified by the *alternative mission* parameter. This means that the AUV can start out in the *adaptive loiter*, and automatically switch to the *adaptive broadside* upon incoming high-SNR contacts. The important parameters for automatic mission switching in the adaptive loiter are therefore the *SNR threshold* and *alternative mission*.

Figure 8 shows a flow diagram of the switching between these two behaviors. As will also be explained in Section 2.3 the AUV starts in a standard loiter. A message is sent via acoustic modem to switch into the adaptive loiter. As explained in the previous paragraph, the AUV then loiters until it observes a contact in the MOOS database with an SNR higher than the *SNR threshold*. The AUV then switches to its *alternative mission*, which is the adaptive broadside behavior.

**Adaptive broadside**

For the adaptive broadside behavior, there are nine parameters. Five of these parameters exist solely for the purpose of switching to other behaviors. These are the *SNR threshold*, *SNR timeout*, *alternative mission*, *run timeout* and *timeout mission*. If the SNR of the

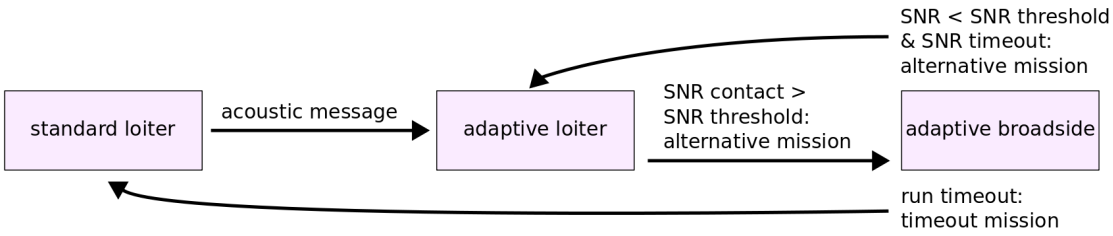


Figure 8: Behavior switching for GLINT09: the AUV starts in a standard loiter, switches to an adaptive loiter upon command, automatically switches to the adaptive broadside upon high SNR contacts, and vice versa on low SNR contacts for an extended period of time, or from the adaptive broadside back to the standard loiter after a global timeout.

retrieved contact is smaller than the *SNR threshold* for the number of sequential contacts (pings) specified by the *SNR timeout*, it will switch to an *alternative mission*. In this case the adaptive loiter behavior was used, as shown in Figure 8. The *run timeout* is a global timeout of the adaptive broadside behavior (specified in seconds or "no-time-limit"), after which it will switch to an alternative mission, parameterized as the *timeout mission* so as not to confuse it with the alternative mission, used when no high SNR contacts are found.

The remaining four behavior parameters are:

- *side*: the side the target is expected on (needs to be predefined because there is no port-starboard discrimination).
- *adaptive angle*: the desired angle between the AUV's (and towed array's) heading and the target position ($0° - 180°$), indicated as `a` in Figure 9 .
- *maximum turn angle*: constraint on heading change per incoming contact, set between $0°$ and $10°$. Introduced to prevent the vehicle from turning sharply and bending the array to the point where the beamforming fails.
- *heading before start*: desired heading at start of the broadside behavior ($0 - 360$ deg).

Two of these parameters were introduced to mitigate limitations of the physical dynamics of the SLITA array. The *heading before start* makes sure the array is straight and the target

is on the expected side before the adaptive broadside takes over. The *maximum turn angle* ensures the towed array is sufficiently straight for line array beamforming.

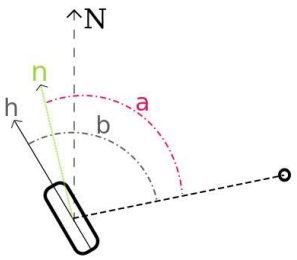


Figure 9: The heading `h` is the angle from the AUV (rounded rectangle) relative to North, the bearing `b` is the angle from AUV to target (circle) and the adaptive angle `a` is the desired angle to the target, which results in a new heading `n`.

When the broadside behavior becomes active, the AUV starts with straightening its array to the *heading before start* value. Once this is done, the bearing to the target, passed from pProcessSlita via the MOOS database (`RELATIVE_BEARING`) to the behavior (Figure 7), is used to calculate a new heading for the AUV. Figure 9 shows an example. The current heading $h$ of the AUV (rounded rectangle) is changed to a new heading $n$, so that the bearing $b$ of the contact (small circle) equals the adaptive angle $a$, which is the desired angle to the contact. This is expressed by the following formulas:

$$n = \left\{ \begin{array}{ll} h + b - a \ , & \text{if } \ side = \text{“right”} \\ h - b + a \ , & \text{if } \ side = \text{“left”} \end{array} \right\} . \tag{3}$$

As has been mentioned, the *side* parameter is needed to define on which side of the array the target is expected due to the lack of port-starboard discrimination. In a more realistic scenario, the port-starboard discrimination could be performed via vehicle maneuvers, or by means of a more complex array configuration. We are currently pursuing both aveneus in parallel for future work.

### 2.3 Mission setup for GLINT09

This section describes specific settings used by the algorithms during the GLINT09 field trials. Parameter values used for the processing as well as the behaviors are provided. Finally, there is a description of the test geometry and expected vehicle path.

Table 1 shows the most important signal processing parameters used during the GLINT09 experiments. Active sonar pings from the acoustic source occurred every 12 seconds and were one second long. Pings were linear frequency modulated (LFM) up-sweeps with center frequency of 2950 Hz and 200 Hz bandwidth. The source level was set to 212 dB re 1 $\mu$Pa. The highest frequency spacing on the SLITA array was used, which provides for half wavelength spacing at 3471 Hz. The acquisition system on-board the OEX recorded data at 6275 Hz sampling rate, a compromise between various acquisition board buffer sizes and desired output file size.

Table 1: Signal processing parameters for behaviour testing during GLINT09

| **Parameter** | **Value** |
|---|---|
| PRI | 12 seconds |
| Ping length | 1 second |
| Modulation | LFM up-sweeps |
| Frequency | 2850-3050 Hz |
| Source level | 212 dB re 1 $\mu$Pa |
| Array spacing (half-wavelength) | 3471Hz |
| Sampling rate acquisition system | 6275 Hz |

Due to the 12 second ping repetition interval, timeseries data for each of the 32 active hydrophones in the array was recorded into 12 second long files. This 12 second data length implies a maximum range limit of approximately 9000 m (assuming 1500 m/s sound speed). Every second ping/file was utilized by the signal processing, while alternate pings were ignored. Just before the GLINT09 sea trial, benchmarking indicated that processing 12 seconds of data required approximately 12 seconds on the vehicle's processing computer. However, given the experimental nature of the trial, the load on the processing stack changed

as various processes were added or removed. Being conservative, utilizing every second data file allowed 24 seconds for the processing to complete. In fact, the trial logs showed that processing during the trial required about 13.5 seconds when the processing stack was fully loaded.

An FFT length of 16384 samples and an overlap of 6375 samples (or 1 second, due to the matched filter of the 1 second long active pulse) was used. This yielded seven overlapped segments per file. A Hanning window was used for temporal windowing to reduce sidelobe ringing. For beamforming, 41 cosine spaced beams were formed. The elements of the array were Hanning shaded for beamforming as well to reduce spatial sidelobes. For both matched filtering and beamforming, frequency bins from 2850-3050 Hz were processed. This was equivalent to a frequency domain bandpass filter around the active pulse band. This was not explicitly windowed or shaded. However, the active pulse itself was windowed in time with a Tukey window 5% on each end, which amounted to frequency windowing for an LFM pulse. This provided adequate de-facto windowing.

Table 2 shows the behavior parameters for the adaptive broadside behavior. The values for these parameters were determined through simulations with processing parameters equal to those given in Table 1. For the adaptive loiter the same *SNR threshold* was used and the *alternative mission* was the broadside behavior. Although for true broadside one would expect an *adaptive angle* of 90°, simulation results showed that delays between data acquisition and the actual turn command, as well as the imposed *maximum turn angle*, meant that a shallower angle was required in order to maintain a circle around the static contact. This will further be discussed in Section 3.

The scenario used to test this behavior is shown in Figure 10. The AUV was set up to start in a standard loiter behavior (black square). A signal was then sent from the command ship via acoustic modem to switch to the adaptive loiter behavior (pink dashed square). The AUV then began to monitor acoustic data for incoming contacts. Once contacts were

Table 2: Parameters for broadside behaviour during GLINT09

| **Parameter** | **Value** |
|---|---|
| side | left |
| adaptive angle | 60° |
| maximum turn angle | 5° |
| SNR threshold | 40.0 dB |
| SNR timeout | 10 potential incoming contacts |
| alternative mission | adaptive loiter |
| run timeout | 800 seconds |
| timeout mission | standard loiter |
| heading before start | 180° |

detected that exceeded the SNR threshold, the AUV automatically switched to the adaptive broadside behavior and began to drive in a circle (pink, dashed) around the contact (the static acoustic source). The *run timeout* parameter was set to 800 seconds, which gave the AUV time to travel a quarter of a circle around the acoustic source before switching back to the standard loiter. The center of the standard loiter was set at the starting location, therefore the AUV returned to that location.

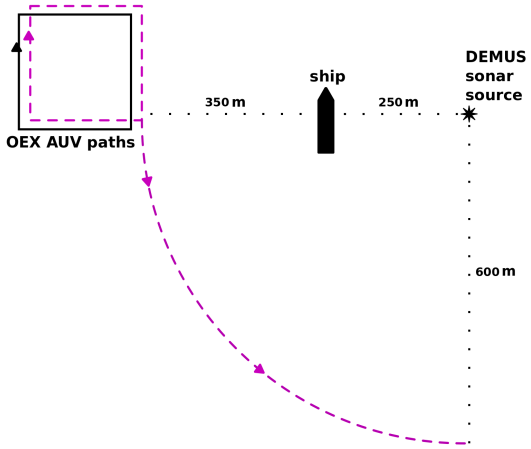


Figure 10: Experimental set-up for the adaptive loiter/broadside behavior test during GLINT09, showing a standard loiter (black square), adaptive loiter (pink dashed square), broadside behavior path (pink dashed quarter circle), the source/target (star), and the research vessel (ship).

This somewhat artificial scenario was used to test the localization and basic detection capabilities of the signal processing algorithm, as well as the broadside behavior responding

to that signal processing. In a more realistic ASW scenario, there are many issues with low SNR target strength and false alarms. These will be dealt with in future developments and improvements in CFAR detection, tracking (which integrates data over time decreasing some false alarms) and tracker tuning, and classification algorithms to distinguish between clutter and targets. These algorithms will exploit the AUV's maneuverability through coupling with vehicle behaviours.

# 3 Results

Figure 11 shows a screenshot of the real-time display, showing a time history of the OEX's path. The square pattern on the top left of Figure 11 was made when the OEX started in the adaptive loiter behavior. During the second lap, while the AUV was on the eastern leg of the adaptive loiter, the acoustic source (DEMUS) was turned on and active pinging began. The OEX detected the active pulse and switched to the broadside behavior. This resulted in the OEX starting to circle the source. The OEX completed approximately a quarter of a circle before the *run timeout* of 800 seconds made it switch to the standard loiter behavior. At that point, the OEX performed a sharp left turn (at the bottom-right side of Figure 11) and began to return to the starting position.

Figure 12 shows the values for relative bearing, retrieved from the MOOS database, that were output by the processing chain during the sea trial. Simulations were run before the trial in order to estimate the best settings for the previously described parameters as well as to test the chosen set-up (Figure 10). Some of these results have been plotted here as well. As predicted in the simulations, the bearing values during the trial asymptotically approach an equilibrium of approximately 100°.

This equilibrium of bearing to target of approximately 100° is much greater than the set *adaptive angle* of 60°. There are two sources of this discrepancy. The first is due to limitations

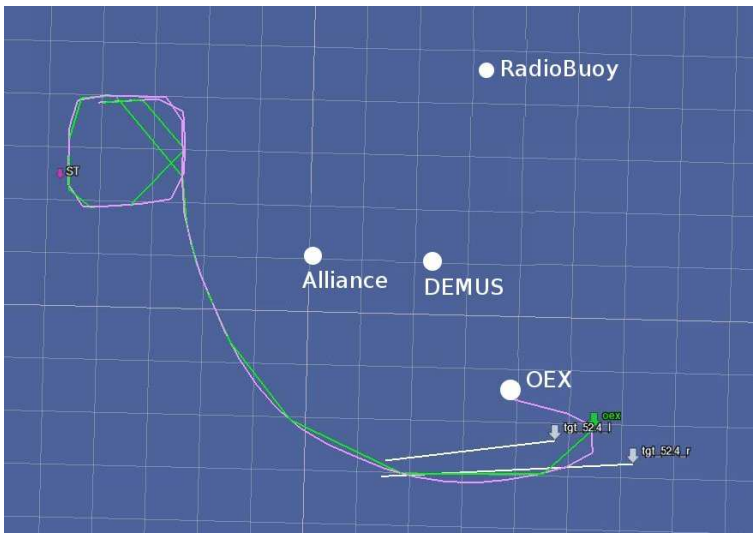


Figure 11: Screenshot of the real-time display during the GLINT09 sea trial test of the adaptive broadside behavior and the adaptive loiter behavior. The OEX's path is shown in green and pink due to different modems used for passing on the position (as can be seen, the pink track (EdgeTech) is updated more often, as it sends location information only). Locations of the Alliance research vessel, DEMUS acoustic source and radio buoy are indicated.

imposed by the maximum turn angle. The second is the effect of the delay between the time when the relative bearing is measured and the time when the heading is corrected. That second delay is at least the 13.5 seconds required to complete the signal processing mentioned in Section 2.3, as well as some small additional time for the computation of the bistatic localization and the behavior processing. These effects were present both in simulation and in the field test.

These ancillary effects may be measured, simulated, and to some extent predicted. The positive result in this test is that the desired behavior of circling the target was achieved. In the future we intend to develop less simplistic behaviors to mitigate these ancillary effects more precisely.

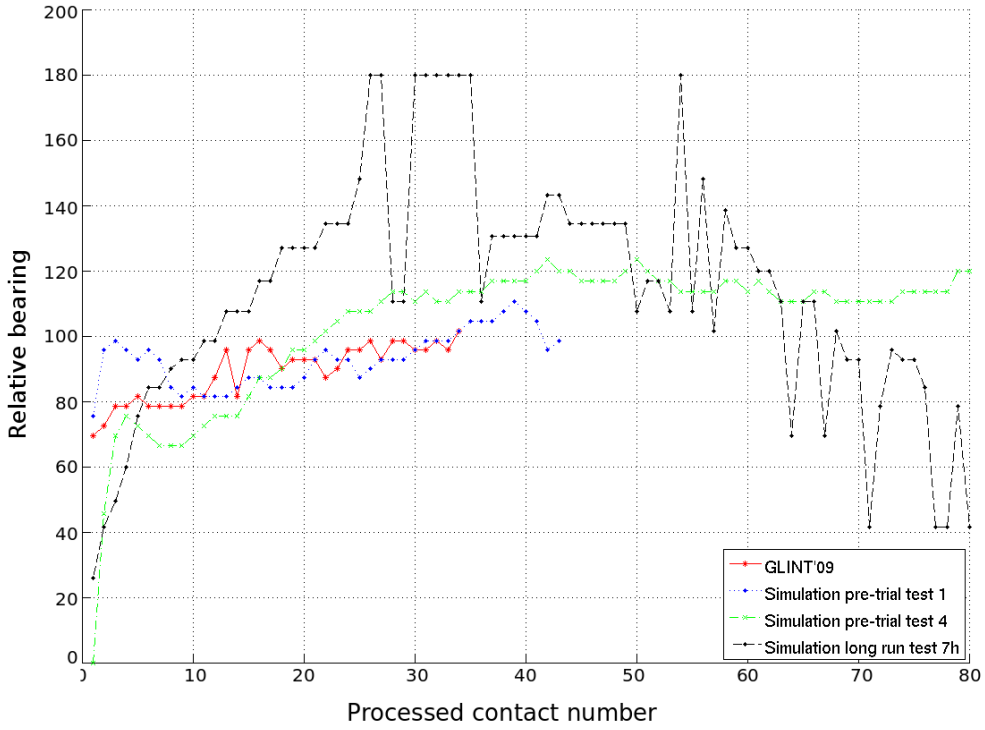


Figure 12: Comparison between relative bearings from the GLINT09 sea trial and several simulations, using the set-up shown in Figure 10. Simulations test 1, test 4 and test 7h encompassed respectively 43, 85 and 948 observations, truncated at 80 for readability.

# 4 Conclusions

Anti-submarine warfare (ASW) has traditionally been carried out by means of submarines or frigates with towed arrays searching for submarines. AUVs are seen as a possible addition to the field of anti-submarine warfare, with the potential of being part of a multistatic active sonar network. Their benefits also include covertness, reduced risk, reduced man power, potential persistence and the ability to optimize sensor position in 3D space based on incoming sensor data. Until now, progress on these systems has been slow because of the challenges concerned with developing sophisticated real-time systems, and having the individual sensors or the system as a whole to act autonomously.

This paper has described the on-board signal processing suite developed for the OEX AUV

at NURC. During the GLINT09 sea trial the adaptive loiter and broadside behaviors were tested on the OEX AUV with a real-time processing payload in combination with the SLITA array and DEMUS acoustic source. The OEX achieved keeping a target at broadside well enough to complete a quarter of a circle around the target. Automatic switching between behaviors, from adaptive loiter to adaptive broadside, and from adaptive broadside to a standard loiter, was also demonstrated.

In summary, this paper has provided a detailed description of the on-board real-time sonar signal processing developed, and shown successful initial adaptive behaviors that operate on the output. To the best of our knowledge, the behaviors demonstrated are the first adaptive behaviors for AUVs in ASW applications that have been reported for a field trial, using real-time on-board processing. These results set the stage for making AUVs more autonomous for ASW applications.

# 5 Future research

For the real-time signal processing, several improvements to the processor need to be put into place to create a more realistic ASW environment. A proper CFAR (constant false alarm rate) implementation with thresholding and detection will be implemented, as well as a tracker. While the active detection and tracking of submarines is a non-trivial matter, NURC will leverage its experience in this field to implement state-of-the-art algorithms to the extent possible in a real time system with limited processing. NURC has these algorithms in house - quick implementation is the only requirement at this point. Indeed, certain speed-ups have already been put into place for the existing signal processing software since GLINT09, resulting in a measured speed-up of almost 30%. Current benchmarks show the we can process a 12 second data file in less than 4 seconds on-board the vehicle.

During the next sea trial, GLINT10, planned for July/August 2010, we intend to test these

signal processing algorithms with improved adaptive behaviors. This will include a more thorough analysis of future simulation performance and characterization of the used and optimum values for the developed behaviors. Specifically, we intend to track a moving echo repeater, as opposed to circling a static, loud source. The echo repeater's level can be adjusted to make the processing and tracking more or less difficult. Primarily, we hope to test behaviors which reach a compromise between keeping the target at broadside (for best localization) and staying close enough to the target to form a contact and hold track.

Future behaviors will utilize new hardware that is being developed at NURC, such as directional arrays. The construction of a second AUV at NURC (from OEX parts), will allow us to begin developing cooperative behaviors. Using the AUVs as homogeneous entities, or perhaps as heterogeneous vehicles with different capabilities.

**Acknowledgments**

This work is funded by the NATO Undersea Research Centre scientific program of work, CASW project. The authors would like to thank the crew of NRV Alliance and CRV Leonardo for their help in obtaining the at-sea data. We acknowledge the great technical assistance and participation during GLINT09 from the staff and students of Massachusetts Institute of Technology (MIT) Laboratory for Autonomous Marine Sensing System (LAMSS), and from the Naval Undersea Warfare Centre (NUWC). Great thanks to Marco Mazzi for his maintenance and care of the OEX AUV, and to Rod Dymond for his construction of the SLITA and upgraded SLITA towed arrays, both of the NURC Engineering Technology Department, and to Arjan Vermeij and Francesco Baralli in the NURC Scientific Department for their programming and technical assistance. S. Kemna would like to thank the Royal Netherlands Navy for supporting her research.

## References

Alvarez, A., Caffaz, A., Caiti, A., Casalino, G., Gualdesi, L., Turetta, A., and Viviani, R. (2009). Fòlaga: A low-cost autonomous underwater vehicle combining glider and AUV capabilities. *Ocean Engineering*, 36(1):24–38.

Bahr, A., Walter, M. R., and Leonard, J. J. (2009). Consistent cooperative localization. In *Proceedings of the IEEE International Conference on Robotics and Automation (ICRA)*, Kobe, Japan.

Baldacci, A. and Haralabus, G. (2006). Signal processing for an active sonar system suitable for advanced sensor technology applications and environmental adaption schemes. In *EUSIPCO 2006*, Florence, Italy. European Signal Processing Conference.

Barkby, S., Williams, S. B., Pizarro, O., and Jakuba, M. (2009). An efficient approach to bathymetric slam. In *Proceedings of the IEEE/RSJ International Conference on Intelligent Robots and Systems (IROS)*, pages 219–224, St. Louis, MO, USA.

Benjamin, M., Leonard, J., Schmidt, H., and Newman, P. (2009). An overview of moos-ivp and a brief users guide to the ivp helm autonomy software. Technical Report MIT-CSAIL-TR-2009-006 http://dspace.mit.edu/handle/1721.1/44590, Massachusetts Institute of Technology, Computer Science and Artifical Intelligence Laboratory, Cambridge, MA, USA.

Benjamin, M. R. (2004). The interval programming model for multi-objective decision making. Technical Report AI Memo 2004-021, Massachusetts Institute of Technology Computer Science and Artifical Intelligence Laboratory, Cambridge, MA.

Benjamin, M. R., Battle, D., Eickstedt, D. P., Schmidt, H., and Balasuriya, A. (2007). Autonomous control of an autonomous underwater vehicle towing a vector sensor array. In *Proceedings of the 2007 IEEE International Conference on Robotics and Automation*, pages 4562–4569, Rome, Italy.

Borgerding, M. (2007). *Streamlining Digital Signal Processing*, chapter Turning Overlap-Save into a Multiband, Mixing, Downsampling Filter Bank. IEEE Press, Piscataway, NJ.

Coraluppi, S. (2006). Multistatic sonar localisation. *IEEE Journal of Oceanic Engineering*, 31(4).

Davies, R. (2006). Newmat C++ matrix library. http://www.robertnz.net/nm_intro.htm.

Ehlers, F. (2009). NURC's multistatic sonar project. Technical Report NURC-FR-2009-03, NURC, La Spezia, Italy. NATO Unclassified.

Eickstedt, D. P. and Benjamin, M. R. (2006). Cooperative target tracking in a distributed autonomous sensor network. In *Oceans 2006*, Boston, MA. IEEE OES.

Eustice, R. M. (2005). *Large-area visually augmented navigation for autonomous underwater vehicles*. PhD thesis, Massachusetts Institute of Technology & Woods Hole Oceanographic Institution, Cambridge, MA, USA.

Freitag, L., Grund, M., Singh, S., Partan, J., Koski, P., and Ball, K. (2005). The whoi micro-modem an acoustic communications and navigation system for multiple platforms. In *Oceans 2005*, Washington, D.C. IEEE OES.

Frigo, M. and Johnson, S. (2005). The design and implementation of fftw3. *Proceedings of the IEEE*, pages 216–231. Also available at: http://www.fftw.org.

Hughes, D., Been, R., and Vermeij, A. (2008). Heterogeneous underwater networks for asw: Technology and techniques. In *Maritime Systems and Technology 2008*, Cadiz, Spain. MAST.

Johnson, D. and Dudgeon, D. (1993). *Array Signal Processing Concepts and Techniques*. Prentice-Hall, Englewood Cliffs, NJ.

Kalwa, J. (2009). The grex-project: Coordination and control of cooperating heterogeneous unmanned systems in uncertain environments. In *IEEE Oceans*, Bremen, Germany.

Kruger, D., Stolkin, R., Blum, A., and Briganti, J. (2007). Optimal auv path planning for extended missions in complex, fast-flowing estuarine environments. In *IEEE International Conference on Robotics and Automation (ICRA)*, pages 4265–4270, Rome, Italy.

Laterveer, R. (2003). Abel multistatic sonar information processing chain. Technical Report Technical Memo RL-JUN03-01, NURC, La Spezia, Italy. NATO Unclassified.

Lum, R., Balasuriya, A., and Schmidt, H. (2009). Multistatic processing and tracking of underwater target using autonomous underwater vehicles. In *Proceedings of the 3rd Underwater Acoustics Measurement Conference*, Nafplion, Greece. Available at http://www.uam2009.gr (accessed 11 December 2009).

Maguer, A., Dymond, R., Mazzi, M., Biagini, S., and Fioravanti, S. (2008). Slita: a new slim towed array for auv applications. In *Acoustics08*, pages 141–146, Paris, France.

Newman, P. M., Leonard, J. J., and Rikoski, R. J. (2003). Towards constant-time slam on an autonomous underwater vehicle using synthetic aperture sonar. In *Proceedings of the Eleventh International Symposium on Robotics Research*, Sienna, Italy.

Pêtrès, C., Pailhas, Y., Patrón, P., Petillot, Y., Evans, J., and Lane, D. (2007). Path planning for autonomous underwater vehicles. *IEEE Transactions on Robotics*, 23(2):331–341.

Poulsen, A. J., Eickstedt, D. P., and Ianniello, J. P. (2006). Bearing stabilization and tracking for an auv with an acoustic line array. In *Proceedings of IEEE/MTS Oceans'06 Conference*, pages 1–6, Boston, MA, USA.

Proakis, J. and Manolakis, D. (1996). *Digital Signal Processing Principles, Algorithms, and Applications*. Prentice-Hall, Englewood Cliffs, NJ, third edition.

Sindt, J.-C. and de Theije, P. A. M. (2003). Target localisation with multistatic systems. In *Proceedings of the 7th European Conference on Underwater Acoustics - ECUA 2004*, Delft, The Netherlands.

Williams, D. (2010). On optimal auv track-spacing for underwater mine detection. In *(to appear) Proceedings of the IEEE International Conference on Robotics and Automation (ICRA)*, Anchorage, AK, USA.

# Document Data Sheet

| Security Classification | | Project No. |
|---|---|---|
| Document Serial No.<br>NURC-PR-2012-009 | Date of Issue<br>May 2012 | Total Pages<br>31 pp. |


Author(s)

Hamilton, M.J., Kemna, S., Hughes, D.T.


Title

Antisubmarine warfare applications for autonomous underwater vehicles: The GLINT09 field trial results.


Abstract

Surveillance in antisubmarine warfare (ASW) has traditionally been carried out by means of submarines or frigates with towed arrays. These techniques are manpower intensive. Alternative approaches have recently been suggested concerning distributed mobile and stationary sensors, such as sonobuoys and autonomous underwater vehicles (AUVs). To field a fully operational system, many technological hurdles need to be overcome. These include battery life, limited acoustic communications ranges, incorporating sonar signal processing on the AUV's embedded hardware, and increasing autonomy to ensure that the system as a whole acts in a sensible and appropriate fashion. The main thrust of this paper is how the latter two issues have been addressed for a real experimental system and how the proposed solutions have been demonstrated at sea. This paper describes ongoing development at the NATO Undersea Research Centre (NURC) to construct an autonomous distributed sensor system that uses AUVs for ASW applications. In a series of at-sea experiments, we have demonstrated real-time processing—incorporating traditional ASW processing as far as tracking—and adaptive autonomous behaviors, which concern AUV navigation to optimize target localization. This paper describes the hardware and software configurations that facilitated the rapid development of this system and details the recent at-sea successes that have been demonstrated with our AUV, towed arrays, and active acoustic sources. Results are given of our most recent at-sea trial, GLINT09, held in the summer of 2009, when an AUV with a towed array detected and maneuvered in response to an active source.



Keywords



Issuing Organization

NURC Viale San Bartolomeo 400, 19126 La Spezia, Italy *[From N. America:* NURC *(New York) APO AE 09613-5000]*

Tel: +39 0187 527 361 Fax:+39 0187 527 700 E-mail: library@nurc.nato.int